Global Scientific JOURNALS

GSJ: Volume 10, Issue 4, April 2022, Online: ISSN 2320-9186

www.globalscientificjournal.com

Topic: PIGGING OPERATIONS IN A NON-BONDED SUBSEA FLEXIBLE PIPE- NUMERICAL ANALYSIS

Authors: **Engr. Gbenga A. Owolabi** (PhD. Eur Ing.CEng CMarEng FIMarEST. ACIArb)
Lead Supply Operations, Supply and Distribution Department
Petroleum Product Marketing Company (PPMC)-Nigerian National Petroleum Limited (NNPC Ltd) Lagos

Engr. Olugbenga Oredeko
Drilling Engineer and Consultant
Houston, Texas

Key words: *Non-bonded flexible pipes, Abaqus, pressurization, depressurization, pigging, blocked, unblocked, hydrate, Sample A &B*

Abstract

The effects of pigging operations in a non-bonded flexible pipe in the oil and gas industries seems to be neglected, but important when the pipeline is blocked by scale, wax, hydrate, sand etc. Pigging is a usual practice where pipeline inspection gauges and devices commonly referred to as pigs or scrapers, are applied to perform various maintenance operations, without stopping the flow of the product in the pipeline.

Pigging is good as a cleaning and inspection tool for pipelines including flexible pipes as it is a usual practice globally. Many often times, operators are compelled to pig by the authority as a statutory requirement for pipelines of certain ages however, considering the benefits, there are a times the flexibles could rupture or burst during the pigging operation, as it scrapes away buildup and debris from the pipes. Though, it helps to improve efficiency of flow and prevent damage to the pipes but can be dangerous if hydrate and other blockages are present in the pipe. This can lead to production shutdown and results into repair cost of multi dollars. Consequently, a research study was carried out focusing on the behaviour of non-bonded flexible pipes with methane hydrate blockage under the influence of diverse load conditions created during pigging operation. A case study applied to a field in the gulf of guinea where a flexible pipe installed early 2000 was blocked and pigging was used to remove it.

To demonstrate in real time, a nonlinear tri-dimensional finite element models were carried out on a seven (7)-layer blocked and unblocked flexible pipe; modelled and simulated. Several studies were conducted to verify the influence of significant parameters on the instability phenomenon when the flexible pipe is under hydrate blockage. The combined load of internal pressure and compressive force was considered as the parameter, and application resulted to a significant change in the stability response of the pipe layers. The obtained results showed the influence of methane hydrate on Sample A (blocked), while Sample B (unblocked) behaves normally under various load conditions.

Introduction

Offshore non-bonded flexible pipe comprises various layers of both metallic and non-metallic materials composition, assembled as a unit structure and commonly used in offshore and deepwater oil, gas, and water as a result of mechanical and chemical properties coupled with its flexibility [1]. The various layers interact freely with each other, static or dynamic wise. A finite element analysis of the behaviour of a typical 6" gas injection flexible pipe, made up of seven (7) layers is used as a case study in this paper.

The referenced flexible pipe was discovered after a comprehensive Remote Operated Vehicle (ROV) survey in a field in the Gulf of Guinea [2].

The failure of the structure was reported late 2010 and was envisaged that the collapse of the flexible pipe was due to continuous pressurization and depressurization process during the pigging operation for the removal of the hydrate plug [3][2].

The schematic of the flexible pipe and the damaged sections is shown in Figure 1 while the functional is presented in Table 1.

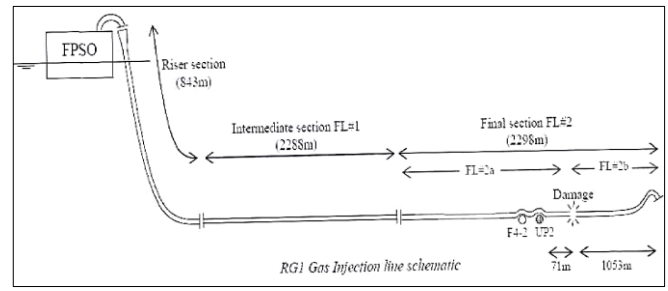

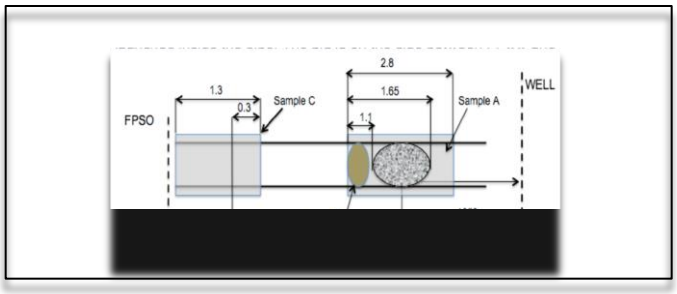

Figure 1: schematic of the flexible pipe and the damaged sections

Table 1: The working properties of the flexible pipe

Properties	Value/Remark
Design type	Gas Injection Flexible pipe (FL2)
Service	Sweet (no H_2S)
Design Pressure	276 bar
Max Operating Pressure	251 bar (227bar)
Design Temperature	80 deg C
Inner Diameter	152.40 mm
Outer Diameter	202.90 mm
Design Life	15 Years
Well water Depth	530 m
Line Length	2298 m
Collapse Resistance	117 bar

Research

Literature reviews on flexible pipes and finite element analysis of non-bonded flexible pipes, damaged and undamaged flexible pipes, including the study on flexible pipe with hydrate blockage under different load conditions were extensively carried out accordingly. The review was done on past papers because modern engineering industries rely heavily on computational models for many purposes, primarily for multiple types of complex failure analysis; and additionally, for optimization regarding design. Also, simulating, fluid dynamics, thermodynamics, and combustion are also critical applications which had been researched in the past, this to give a clear direction on this present work. Some of these works by great scientists are but not limited to:

J. de Sousa, Paulo F. Viero, Carlos Magluta N. Roitman and R. Motta. In June 2010, De Sousa et al. dealt with a nonlinear three-dimensional finite element (FE) model capable of predicting the mechanical response of flexible pipes subjected to axisymmetric loads focusing on their axial compression response. Moreover, to validate the model required experimental tests, which were carried out at COPPE/UFRJ. In these tests, a typical 4" flexible pipe was subjected to axial compression until it failed with radial and axial displacements measured and compared to the model predictions. The excellent agreement between all obtained results indicates that the proposed FE model efficiently estimates flexible pipes' response to axial compression. [1]

Roberto Ramos Jr. and Alexandre Kawano, in 2015 analyzed numerically a 2.5" flexible pipe subjected to traction and internal pressure. The effect of internal and external pressures on the displacement of flexible pipe, when subjected to axisymmetric loads, was discussed. A typical example is presented in Figure 2 [6].

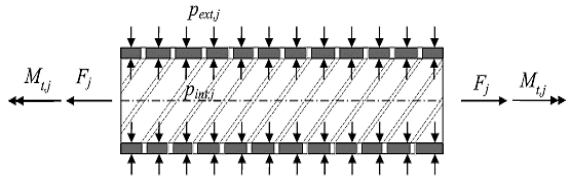

Figure 2: Load applied to the boundaries of a plastic layer [26]

Traction force supported by the layer (Fj)

- Twisting moment supported by the layer (Mtj)
- Internal pressure applied on the internal cylinder surface (pintj)
- External pressure applied on the internal cylinder surface (pextj)

Gabriel Gonzalez, Jose Renato Mendes des Sousa, and Luis Sagrilo presented in 2015, a finite element model, entirely developed in ABAQUS® environment, fully capable of calculating stresses and strains in those several layers when subjected to different types of loads.

The analyses considered the variation of normal contact stiffness (nk) and coefficient of friction (μ)

which were chosen from 10-10^5 (μ = 0.10) and 0.03-0.13 (nk= 5000) for Normal stiffness and coefficient of friction. The best

parameters that give the desired result are when the friction coefficient is 0.10 and contact stiffness is 1000 N/mm3 [4].

Ben Edmans, Dinh Chi Pham, Zhiqian Zhang, Tianfu Guo, Sridhar Narayanaswamy (2014), Edmans et al. introduced a new multiscale approach for the analysis of FE flexible pipes. The primary focus is on the prediction of failure modes and increases in design life against hydrostatic loading. This paper conclusively shows ordered multiscale designs for flexible pipe model, with evidence of hybrid beam FE implementation in a two-dimensional (2D) system. Accordingly, further works should be focused on "implementing a three-dimensional hybrid beam element and creating a fully nested computational procedure", with considerations of global and local systems [5]. Generally, the above literature reviews on non-bonded flexible pipes shows no research study focused on the hydrate blockage in flexible pipes and their consequent failures.

Finite Element Modelling Steps

ABAQUS software was selected to perform the analyses out of diverse software packages. The steps are clearly explained in this paper [7].

Geometry & Element

Considered is a typical 6" (152.4 mm) flexible pipe, which was developed to analyze primary layers' geometric properties, including the pipe layer specification and material properties. The layers were modelled in 8-noded SOLID C3D8R element as represented in Figure 3 and parts shown in Table 2. The result is consistent at the end simulation. The standard solid element is a solid model where the material is represented throughout the component or structure.

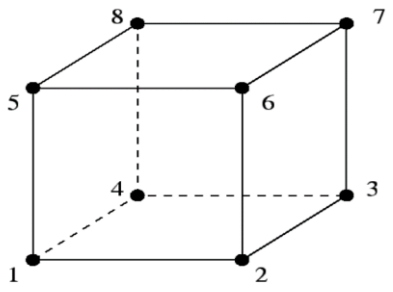

Figure 3: 8-Nodes linear brick Element (C3D8R) [44]

Table 2: Non-bonded Flexible Parts, Model 1-C3D8R

Layer	Type	Material	Element Type
1.	Carcass	Metallic	Solid
2.	Pressure Sheath	Non-Metallic	Solid
3.	Zeta/Pressure Armour	Metallic	Solid
4.	1st Tensile Armour	Metallic	Solid
5.	2nd Tensile Armour	Metallic	Solid
6.	High Strength Tape	Non-Metallic	Solid
7.	Outer Sheath	Non-Metallic	Solid
8.	Methane Hydrate	Hydrate	Solid

The manufacturer supplied the geometry of the flexible pipe under consideration as presented in Table 3.

Table 3: Flexible Layers geometry Properties

Layer	No. Layer description	H	r_i	r_o	r	Lay angle
		(mm)	(mm)	(mm)	(mm)	(α^o)
1	Interlocked carcass, 48.0 x 1.0 AISI 304 (FE) 20	5	80.03	85.03	82.53	87.6
2	Internal plastic sheath RILSAN P4 0TL TP01	4	85.03	89.03	87.03	
3	Zeta-clip, 2 tendons th 6.2 FM 35 (FI 11)	6.2	89.03	95.23	92.13	85.6
4	First Armour Lay 35.0 deg FI41 2x7mm, 40 wires	2	95.23	97.23	96.23	35
5	Second Armour Lay -35.0 deg FI41 2x7mm, 44 wires	2	97.23	99.23	98.23	-35
6	High Strength Tape 1 Tape-BA09 KV 400daN130mm	1.25	99.23	100.48	99.855	
7	External Sheath FINATHENE (TP 04)	4.8	100.48	105.28	102.88	

r_i Internal Radius

r_o Outer Radius

r Mean Radius

Material Properties

The material properties of the flexible pipe under consideration are given in Table 4.

Table 4: Flexible Pipe material data based on the equivalent orthotropic materials

Layer	Layer description	UTS (MPa)	SDP (MPa)	Mass (kg/m)	I.D. (mm)	h (mm)	Area (mm)	E (MPa)
1	Interlocked carcass, 48.0 x 1.0 AISI 304 (FE) 20	550	-	11.70	160.05	1.17	19.6	16507
2	Internal plastic sheath RILSAN P4 0TL TP01	48	-	2.31	162.40	6.42	-	345
3	Zeta-clip, 2 tendons th 6.2 FM 35 (FI 11)	1000	380	22.73	175.23	3.78	54.1	13692
4	First Armour Lay 35.0 deg FI41 2x7mm, 40 wires	1400	403	8.27	182.80	2.00	-	345
5	Second Armour Lay -35.0 deg FI41 2x7mm, 44 wires	1400	461	8.39	186.80	2.00	-	20500
6	High Strength Tape 1 Tape-BA09 KV 400daN130mm	3400	-	0.40	190.80	1.25	-	345
7	External Sheath FINATHENE (TP 04)	34	-	2.81	202.90	4.80	-	20500

Regarding the study, the layers were modelled in isotropic geometric except for the carcass and the pressure armours modelled as orthotropic properties type. The flexible pipe data presented in Table 4 with new equivalent material thickness is

used for the analysis. The carcass and the pressure armour layers are replaced by an equivalent material and geometric orthotropic layers because of the computational solution time of modelling the three-dimensional layers. However, the overall flexible pipe thickness remains the same. The exact material property of the equivalent orthotropic layers for the carcass and pressure armour, including the results from the embedded orthotropic sheath layer, are wholly considered in the present work.

General Mesh

The typical finite element mesh of the individual flexible pipelayers is shown in Figure 18 with global seeds of approximately global size curvature control of maximum deviation factor of 0.1 and minimum size control by a fraction of global size 0.1 applied. This was applied to all seven (7) layers, including the plug/blockage. The effects of different element sizes in the cross-section of the pipe layers were examined to provide accurate results at a reduced computation time. The layers were finely meshed and observed for better results. The number of the element was carefully chosen so that the aspect ratio of the elements was as close to one as possible. Therefore, mesh sensitivity analyses were performed to verify the number of elements in each of the parts. Abaqus/Explicit is used to determine which slave nodes in the predicted configuration penetrate the master surfaces to prevent penetration of layers in the radial direction. Table 5 shows the mesh sensitivity analysis with the problem size, which includes the total number of elements, nodes and variables in the assembly that is large enough to provide better results and Figure 4 denotes the mesh structures.

Table 5: Mesh sensitivity analyses- Problem Size

Parts	No of Elements	No of Nodes	Total No of Variables
Solid	53,599	118,039	267,033
Shell	60,343	99,165	273,117

The total number of solid and shell parts elements is 53,599 and 60,343, respectively, while the node is 118,039 and 99,165 for both solid and shell elements.

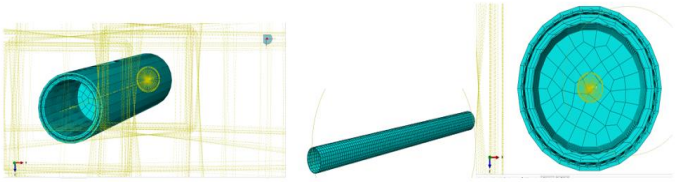

Figure 4: Meshed Solid Elements

Assembly Of Non-Bonded Flexible Part Layers

The layers are assembled along the normal axis, and the tensile wires were initially arranged with coaxial constrained of the tendons to form a complete spiral pipe. The process is shown in Figure 10 with the first tensile 40 tendons and the second tensile with 44 tendons/wires, while the same Figure 10 shows the entire parts assembly.

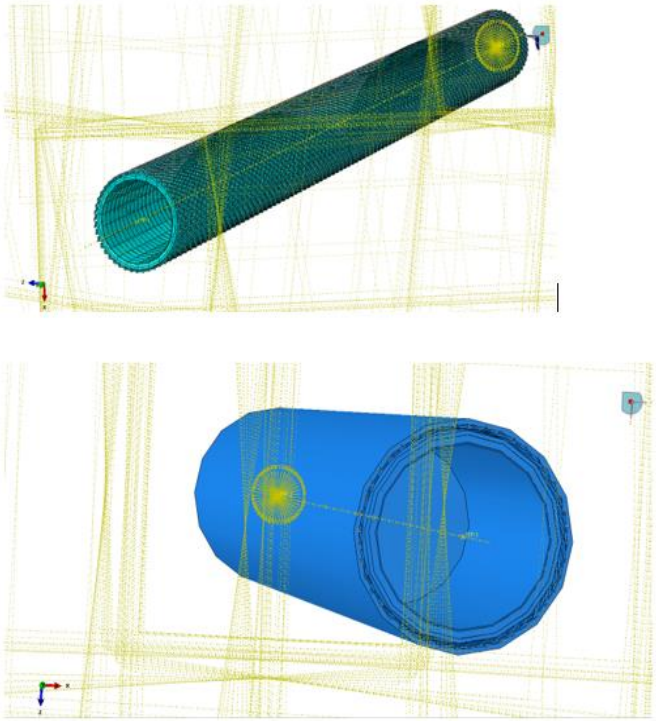

Figure 5: Assembled parts

Interactions And Constraints

General contact algorithm in Abaqus/Standard explicit, which is surface to surface contact formulation, was used for all layers. Two surfaces, surf 1 and surf 2, were created each for the parts, and the contact domain contains surface pairs of a master and a slave. For the numerical simulations, it is normal behaviour, pressure overclosure: hard contact, constraint enforcement method by default, and allow separation after contact was adopted. Otherwise, pressure overclosure: Linear, constraint

enforcement method by default with contact stiffness of 10^{-5} was adopted while frictionless was adopted in tangential behaviour-friction formulation. Please see Figure 6.

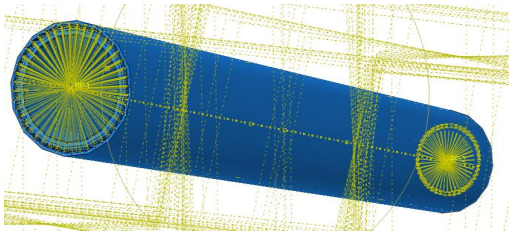

Figure 6: Application of constrained points RP-1 and RP-2

Load Cases and Boundary Conditions

The simulation investigates the influence of the load case in Table 6 but only focused on case 4 in this paper for samples A and B:

Table 6: Load Cases and Boundary Conditions

Load Case	Load Type	Boundary Conditions
1.	Internal Pressure (IP)	One end (RP-1) is constrained in all directions using Encastre, while end 2 (RP-1) is free
2.	Compressive Force (CF)	
3.	External Pressure (EP)	
4.	Internal Pressure + Compressive Force (IP+CF)	
5.	Coefficient of Friction (CF) + Contact stiffness (CS)	Varied CF+ constant CS

Subsequently, for all the load cases, the essential boundary conditions were defined one end fixed while the other pipe end was free.

Blockage Simulation

Hydrate blockage ranges from diameters 0.1 to 1 m length were introduced into sample B and simulated with tangential behaviour, penalty, and normal behaviour of stiffness constant 10^{-5}. The results show a significant decrease in the displacement and high-stress concentration in all directions in the flexible pipe. The impact of the blockage/plug reflected more in the values of mises stress, reacting force, and hoop stress on the entire structure, especially the carcass and the tensile wires. The plug is constrained at point RP-1 with the other two sides fixed, so there is no significant movement. The relocation vis-à-vis movement started with an increase in internal pressure. Table 7 shows the applied plug parameters while Figure 7 shows the plug structure as the formation is explained by Kvenvoden [10] .

Table 7: Simulated Blockage (Plug) Sizes

Length (m)	Inner diameter (mm)
0.1	0.00762
0.5	0.0381
1.0	0.0762

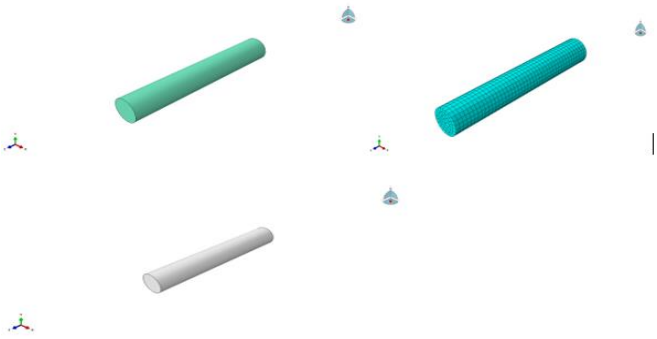

[10]

Figure 7: Meshed and unmeshed blockage/plug

General Simulation and Modelling

A geometrically non-linear problem was analyzed, and the non-linearity resulting from the contact surfaces presence, including the rigid body that produces large displacement in the tensile layer. Elements are distorted from their original shapes as the deformation increase along the pipe axis. All elements are of acceptable shape concerning aspect ratio and others by carefully monitoring the hourglass energy to internal energy around 5%. A complete blockage of tangential behaviour, penalty, and normal behaviour of stiffness constant 10^{-5} shows a significant decrease in the displacement and high-stress concentration in all directions in the flexible pipe. It is clearly shown that the plugin of the flexible pipe imparts more von mises stress, reacting force and hoop stress on the entire structure, especially the carcass and the tensile wires. There is no significant movement of the plug because the two ends were fixed and constrained to reference point 1 (RP-1); and the relocation started with increased internal pressure. The analysis considered the effects of large deformations and rotations. The non-linear effects were ignored when validating the results. Consequently, the magnitude of loads in all cases was kept practicably within the allowable values to ensure that the resulting strains were kept within elastic limits.

Applied Boundary Factors and Load Values

As earlier mentioned, the ends boundary conditions were imposed through reference points RP-1 and RP-2 located at

both ends of the pipe segment. One end RP-2 is constrained at all points while RP-1 is free. Coupling the end nodes of the elements in six degrees of freedom with the reference node simulated the axial and radial constraint of the end fitting. At the end 1, the layers were constrained in all directions using Encastre, while at End 2, the layers are constrained to a reference point RP-1. Figure 8 shows the applied boundary condition (BC) as described.

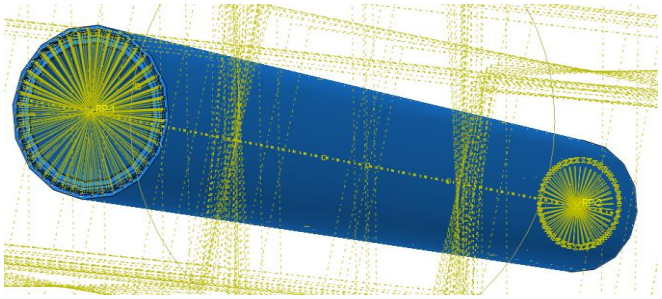

Figure 8: Application of constrained at points RP-1 and RP-2

Applied load values

The influence of the combined compressive force and Internal Pressure loads were analyzed on samples A and B with the magnitudes shown in Table 8:

Table 8: Loading values

Load Type	Load Value
Internal Pressure + Compressive Force (IP+CF)	22.7 MPa + 1747.79 kN

Internal Pressure + Compressive Load

The applied load is a combined internal pressure and compressive force from 22.7 to 65.4 MPa and 1747.79 kN under the same conditions. The results were significant as they show a considerable difference as expected in sample A than sample B.

Effect of Co-efficient of Friction

The coefficient of friction for the interaction and surface contact was varied from 0.1 to 0.5, and the contact stiffness was kept constant throughout the simulation. The results obtained showed that the higher the coefficient of friction, the lower the stress concentration or, the lower the coefficient of friction, the higher the stress when the coefficient of friction μ =0.5, the stress values obtained for Sample A is higher than sample B and same applicable to displacement and reaction force, which were due to the hydrate presence.

The values obtained for sample A is higher than sample B for stress, displacement, and reaction force due to the hydrate being blocked for all the load conditions.

Results and Discussions

The Stress analysis was performed on the hydrate blocked flexible pipe specimens in accordance with the case study [3] and the manufacturers given data. This includes but not limited to the following [2]:

- Operating Pressure 22.7MPa
- Compressive force 1747.79 kN

The concentration of stress in the layers particularly the two tensile wires are critically studied. Internal pressure 22.7MPa was applied at the inner surface of the carcass and on the hydrate plug and the stress analyses performed with proper boundary conditions and loads.

The analysis shows that the layers of the flexible pipe under investigation most especially the tensile wires are highly sensitive to the applied load. The response of the pipe to the subjected load shows a significant deformation which indicates the presence of the plug in the pipe triggers the failure modes stated in API 17J [8].

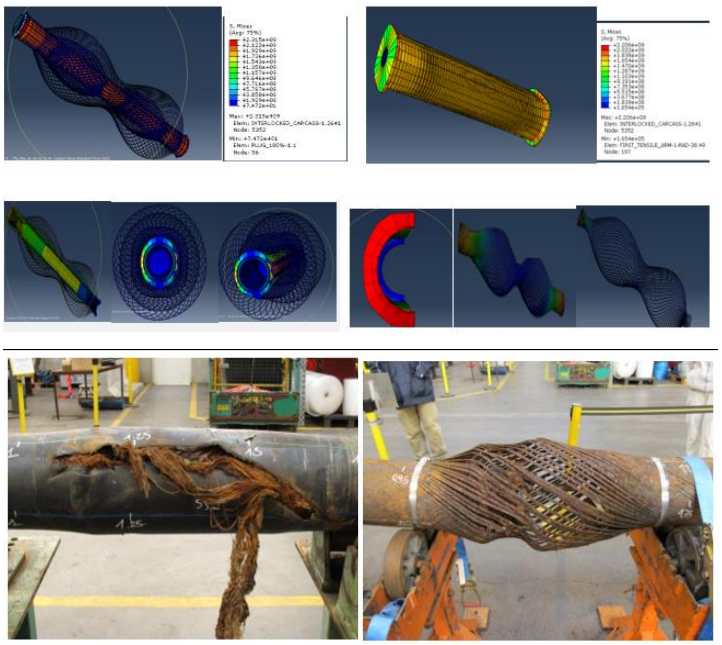

Figure 9: Pipe deformations and the pipe under investigation with the same deformation with simulated pipes ***Error! Reference source not found.****[3]*

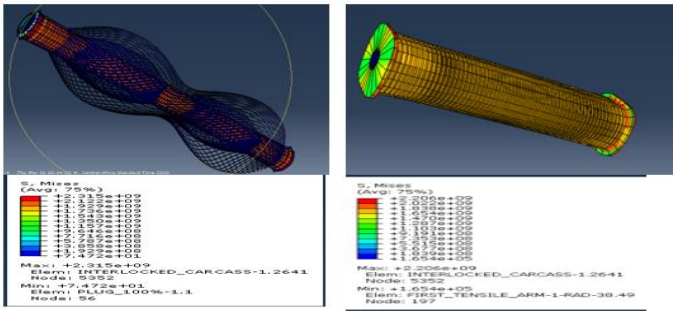

Figure 10: Deformations (a) the hydrate blocked flexible pipe layers; (b) unblocked flexible pipe under a combined load

Load case : Internal Pressure and Compressive Force

A combined load of 22.7 MPa internal pressure (IP) was applied to the inner surface of the carcass, and a 1m long hydrate plug, and a 1747.79 kN compressive force (CF), was simultaneously placed on the reference point RP-1. However, the deformation in Sample A, a hydrate blocked flexible pipe, was higher than expected. The first tensile wire was twisted at the middle, and the ends narrowed in diameters; the deformation at the two points of the first tensile wire resembled a birdcage that is ready to burst. The second tensile wire looks like a balloon ready to burst and resembles the first tensile wire deformation presented in Figure 11. The reacting force is 25.76% greater than the applied tension value, which shows that the hydrate blockage created much more load in the pipe, resulting in its deformation. The average deformation of 0.1852 mm, approximately 0.66% of the original length, is due to the higher value of the hoop stress, which was earlier confirmed by lame's and normal equations and the reaction force. The deformation is higher than the flexible pipe without blockage, which stands at an average of 0.1474 mm, representing 0.53% of the pipe's original length of 2.8 m. The stress components (MPa) and the strain are shown in Graphs 1 and 2, with the stress pressure having a higher value than the von mises and maximum stress. The hoop stress is negative, which denotes that the stress is acting outwardly on the circumferential part of the pipe. The overall result is shown in Table 9.

Table 9: Overall Result of Stress when applied a combine load

Int. Pressure + Compressive force	Frictionless, stiffness constant=0.00001					
Reacting Force (kN)	2198			1748		
	Blocked Flexible Pipe			Unblocked flexible Pipe		
Load type	S_{mises} (MPa)	S_{22} (MPa)	U (mm)	S_{mises} (MPa)	S_{22} (MPa)	U (mm)
Carcass	2315	1574	0.129	2206	1574	0.1035
Pressure Sheath	4.341	0.1435	0.127	3.452	0.114	0.1013
Zeta Pressure Armour	628.8	*0.002708	0.1274	50	*0.002153	0.1013
First Tensile	3.328	1.484	0.1275	2.647	1.180	0.1014
Second Tensile	8.861	0.410	0.1854	7.046	0.326	0.1474
High Strength Tape	532	27.89	0.1274	423.1	22.18	0.1013
External Sheath	3.857	0.288	0.1274	3.067	0.229	0.1013

Consequently, for considering the load condition, it is observed that the deformation and stress distribution is greater when the pipe is under a combined load, that most often occurs under internal pressure and compressive force. The simulation has shown that a blocked flexible pipe apart from being sensitive to load, is also liable to damage or failure modes as recommended in API 17J [9]

Graph 1: Sample-A: Stress distribution in Carcass layer

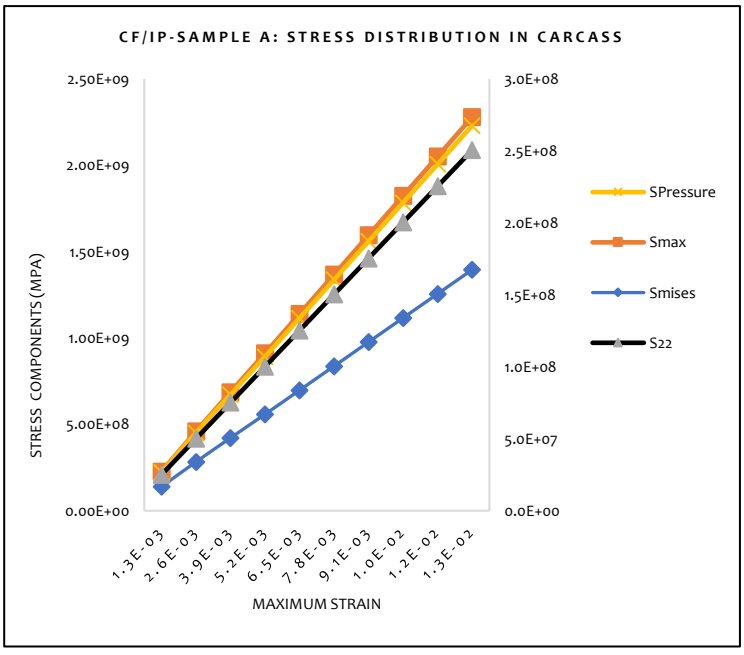

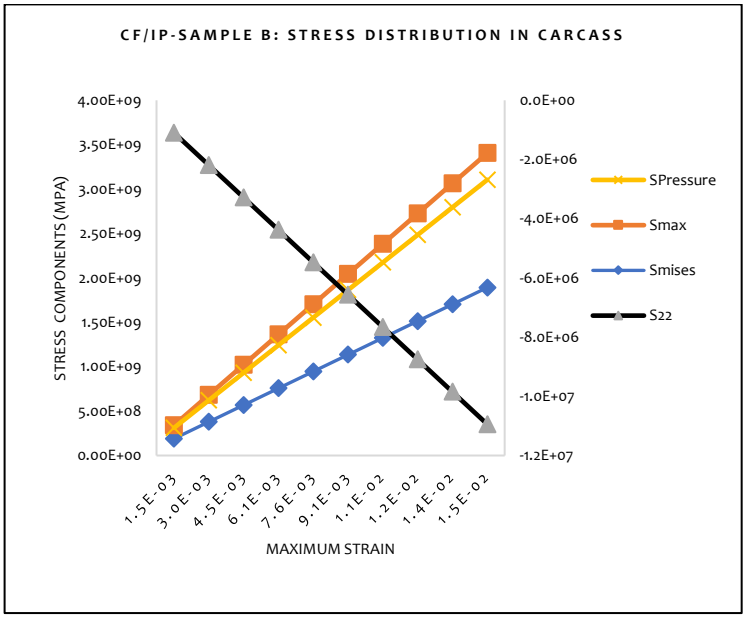

Graph 2 Sample A: Stress distribution in Tensile Wire layer

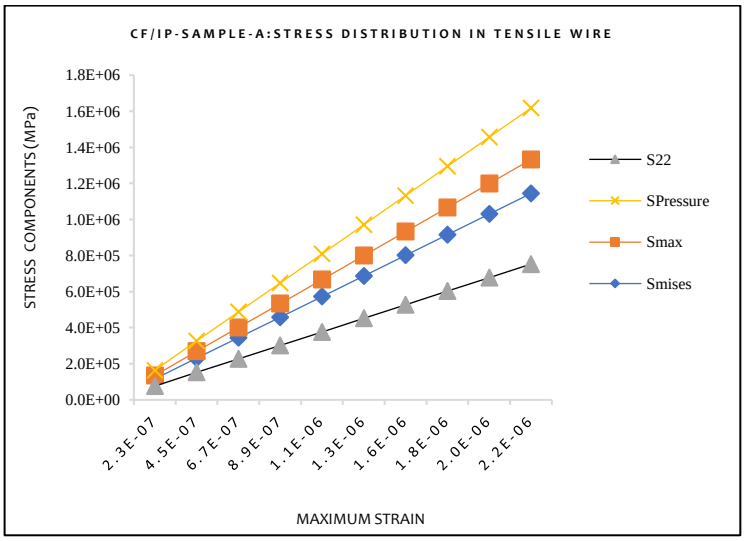

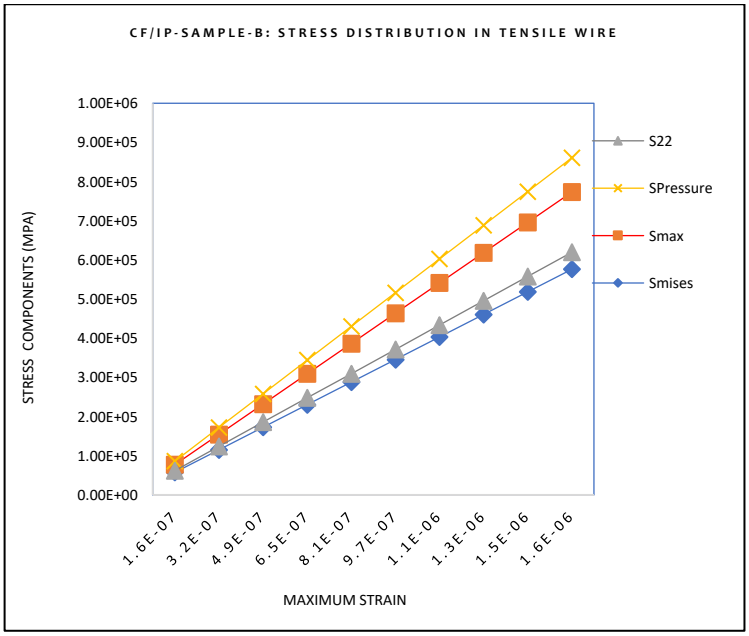

Reaction Force vs Displacement

The numerical models were simulated using the available data by subjected to various load conditions and defined boundary factors as prescribed by the real-world physical condition. The results obtained from the non-bonded flexible pipe samples A and B showed a general effect of blockage on the flexible pipe, which no research has mentioned. While sample A is blocked pipe, sample B is unblocked pipe, and the results obtained varied significantly along the length and the wall thickness of the two samples, as shown in Figure 9 for the reaction force and displacement. The concentration of stress is much more in Sample A compared to Sample B. The presence of blockage/plug in the flexible pipe creates more stress in the layers. The stress and reaction force increased with an increase in the internal pressure from operating pressure to burst pressure. The operating pressure is considered the pipe normal behaviour and could only be experienced, verified, and validated under pressure ranges from 22.4-25.4 MPa. The stress distribution along the length of the pipe and the wall thickness showed higher values in Sample A than in Sample B. However, it is noted that the plug absorbs part of the stress in Sample A. The pipe ruptured mainly due to the block trying to adjust the stress level. In addition, the coefficient of friction impacts significantly on sample A, compared to sample B for stress, displacement, and reaction force due to the hydrate being blocked. The lower the coefficient of friction, the higher the stress values. This shows that the pipe responds to the coefficient of friction. The summary is presented in Table 10.

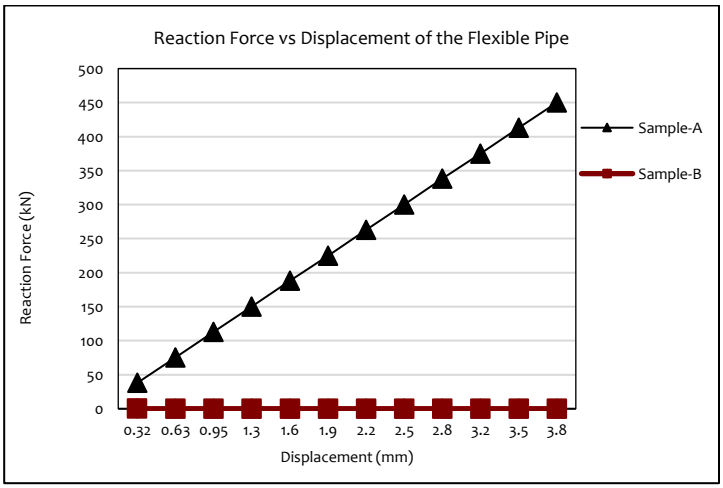

Figure 11: Reaction Force and Displacement in Samples A & B

Table 10: Numerical stress values when applied a combined load

Compressive Force + Internal Pressure (CF+IP)		Sample A	Sample B
Layers	UTS (MPa)	Stress Mises (MPa)	Stress Mises (MPa)
	Designed	CF+IP	CF+IP
Carcass	550	2315	2206
Pressure Sheath	*48	4.34	3.45
Zeta-Pressure Armour	1000	628	50
First Tensile Armour	1400	3.33	2.65
Second Tensile Armour	1400	8.86	7.05
High Tensile Strength	*3400	532	423
External Sheath	*34	3.86	3.07

* Source from the internet

Conclusions and Recommendation

The results showed that the hydrate formation or any blockage/plug generates excess loads on the non-bonded flexible pipes wall in static and dynamic positions, as shown in Figure 12. This produces unnecessary stress that damages the flexible layers while the deformation of tensile wires in birdcage form is because of the excess loads created and impacted by the hydrate plug/blockage. As observed, the estimated load to tear the layers is carcass- 77 kN, pressure sheath- 63 kN, and others swell up with an additional 10 kN. However, the analysis shows the reaction force in the hydrate blocked pipe to be 450 kN, which is much more than the load impacted during the 1st, 2^{nd,} and 3rd pressurization at 87 kN, 269 kN 318 kN, respectively. Subsequently, the loads induced by the hydrate plug are higher than the compressive load that can lead to birdcage of the tensile wires and tears the carcass and the pressure sheath, with an indication in the models. The rupture of the non-bonded flexible pipe under investigation is due to the process (continuous pressurization and depressurization) that lead to the removal of the hydrate. It is essential to mention that the investigated flexible pipe is susceptible to load. The pipe's collapse or deformity was because of the compressive axial load generated by the pressure created during the pigging process. The values of numerical tensile stresses are lower in all the layers except for the carcass. It implies that the load transmits from the inner layer to the outer layer; however, these loads with the excess reaction force generated, which for internal pressure is 450 kN and for a combined load is 2198 kN damaged the flexible pipe. In conclusion, the applied loads damaged the non-bonded flexible pipe, under investigation by this research work. This shows that loads during operation can have adverse effects on the pipe layers and can eventually lead to damage if not carefully handled. It is recommended according to API 17B [9] that the blocked pipe be handled with utmost care while pigging or during any attempt to remove the plug/blockage, be hydrate formation or wax. This, if not well handled, could permanently deform the flexible pipe, and perhaps damage it.

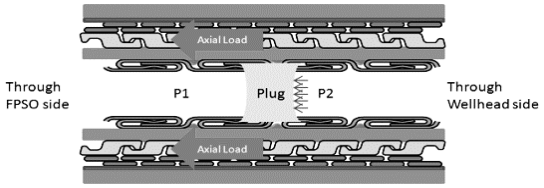

Figure 12: General effects of plug in the investigated pipe

Finally, the presence of the plug in the flexible pipe resulted in the differential pressure at the plug location (depressurization) and created an axial load in the flexible pipe layers. The failure analysis is entirely consistent with experimental investigations and supported by additional assessments. Failure was not due to manufacturing, material properties, installation, ageing, or corrosion. The failure mechanism based on the analysis are as follow:

1. Birdcage of armour wires was because of the presence of hydrate plug
2. Unlocking of the Zeta layer during pressurization was due to hydrate dissolution
3. Tearing of the carcass linked to the presence of a hydrate plug
4. Attempt to pressurize the line following hydrate dissolution leading to failure of pressure sheath.

The outcome shows that the blockage inside the flexible pipe exerts more loads on the layers, which can damage the pipe and lead to eventual failure. The pipe with blockage is handled with caution by following the operation guideline during the removal process or during an attempt to remove the plug/blockage, such as hydrate or wax formation. Without laid down procedures, any attempt could permanently deform the flexible pipe and perhaps result in a replacement or dump on the seabed. The problem can be avoided based on the outcome of this research work, with identified ways to avert damage to the flexible pipes should there be a blockage.

REFERENCES

[1] J. de Sousa, J. R. M., Viero, P. F., Magluta, C., Roitman, N. Motta, A. M. R. An Experimental and Numerical Study on the Axial Compression Response of Flexible Pipes. In; June 6-11, 2010; Shanghai: ASME 2010 29th International Conference on Ocean, Offshore and Arctic Engineering OMAE 2010.

[2] I Clement, E Godefroy and others, 2014 Abo 5 6" GI flowline expertise and failure analysis_ 26_05_2014.

[3] ENI flexible pipe final workshop 26.05.2014 POLIMI.

[4] Gonzalez G. M., De Sousa J. R. M., Sagrilo L.V.S. An unbonded flexible pipe finite element model. In Proceedings of 36th Ibero-Latin America Congress on Computational Methods in Engineering, 22-25 November 2015. In; 2015; Rio de Janeiro.

[5] Ben Edmans, Dinh Chi Pham, Zhiqian Zhang, Tianfu Guo, Sridhar Narayanaswamy, G. S. (2014) 'Multiscale Finite Element Analysis of Non bonded Flexible Risers', *Proceedings of the ASME 2014 33rd International Conference on Ocean, Offshore and Arctic Engineering*, OMAE2014-2, pp. 1–9.

[6] Roberto RamosJr. A. Local structural analysis of flexible pipes subjected to traction, torsion and pressure loads. Marine Structures. 2015; 42: 95-114.

[7] Simulia. ABAQUS 16.4-4 Online Documentation. http://abaqus.software.polimi.it/v6.14/index.html

[8] API, July 2008, Specification for Unbonded Flexible Pipe, API RP 17J, American Petroleum Institute, 3rd ed, New York.

[9] API, July 2008, Recommended Practice for Flexible Pipe, API RP 17B, American Petroleum Institute, 4th ed, New York

[10] Kvenvolden, K.A..L., 2001. The global occurance of natural gas hydrate. *Natural Gas Hydrates: Occurance, Distribution and detection*, pp.3-18.